Journal of Theoretical and Computational Chemistry
Vol. 16, No. 5 (2017) 1750046 (15 pages)

DOI: 10.1142/S0219633617500468

World Scientific
www.worldscientific.com

Formation of a pre-reaction hydrogen-bonded complex and its significance in the potential energy surface of the $OH + SO_2 \rightarrow HOSO_2$ reaction: A computational study

Vijay M. Miriyala, Priya Bhasi, Zanele P. Nhlabatsi
and Sanyasi Sitha*

Department of Chemistry
University of Johannesburg
P.O. Box 524, Auckland Park
Johannesburg 2006, South Africa
**ssitha@uj.ac.za*

Received 12 April 2017
Accepted 14 June 2017
Published 5 July 2017

Using computational calculations, we have revisited the potential energy surface (PES) of the reaction between OH and SO_2, which is believed as the rate-limiting step in the atmospheric formation of H_2SO_4. In this work, we report for the first time the presence of a pre-reaction hydrogen-bonded complex between OH and SO_2 in the reaction PES. Based on this finding, it has been shown that the reaction can be considered as a two-step process in which the first step is the formation of the pre-reaction complex and the second step is the transformation of this complex to the product. It was observed that due to the presence of this pre-reaction complex as a potential well in the reaction PES, the barrier height got increased by around two-fold for the second step. Based on this observation, it has been proposed that the kinetics of the reaction is going to be affected. Also based on the analysis of the geometries of this pre-reaction complex and the transition state, it has been argued that the step involving the transformation of this pre-reaction complex to the product via the transition state is going to be the slowest step as this transformation involves large structural changes of the stationary points involved.

Keywords: Sulfuric acid; H_2SO_4; SO_2; $HOSO_2$; OH-OSO pre-reaction hydrogen-bonded complex; potential energy surface.

1. Introduction

Sulfur dioxide (SO_2) is one of the key species that determines the aerosol content of the troposphere and stratosphere, and gaseous sulfuric acid (H_2SO_4) has been identified as a key precursor in the nucleation process because of its low vapor pressure at typical atmospheric temperatures. Atmospheric aerosols formed by nucleation of vapors of H_2SO_4 affect the radiative forcing and thereby the climate change. The reaction of OH with SO_2 to form hydroxysulfonyl radical (Reaction 1)

*Corresponding author.

is the first step in the formation of sulfuric acid in the atmosphere.[1–5] Being the rate-determining step,[1–5] kinetics of this reaction is studied extensively both experimentally and theoretically[3,6–16]:

$$OH + SO_2 \rightarrow HOSO_2 \quad \text{(Reaction 1)}.$$

Recent developments in this field also show that besides the OH, there is another important oxidant for the SO_2 oxidation in the atmosphere known as Criegee intermediate, which is also responsible for substantial contribution to atmospheric H_2SO_4 formation.[17–20] Due to strong atmospheric implications of this reaction, many recent studies have been focussed on this Criegee intermediate[18–20] and its reaction with SO_2.[18] In the past, there were many attempts to find a barrier to this reaction,[21,22] and a more detailed discussion about those can be found in one of the recent reports by Sitha *et al.*[23] Also, in the report of Sitha *et al.*, they have shown a considerable barrier of ∼5.0 kcal/mol for the first time for this reaction using MP2=Full/6-31++G(2df,2p) method.[23] This present work is focussed on revisiting the potential energy surface (PES) of the reaction between OH and SO_2 using quantum chemical calculations. Revisiting this important reaction PES, we noticed the presence of a very stable hydrogen-bonded complex between SO_2 and OH as a pre-reaction potential well between the reactants and transition state. As incorporation of this stable complex is very much crucial for the complete and accurate representation of the PES of this reaction, in this work we have attempted to do so and also discuss its implications.

2. Computational Methods

All quantum-chemical calculations have been performed using Gaussian 09 package, and the geometries of all the stationary points in the PES have been visualized using GaussView program.[24] In this work, MP2(full) calculations[25,26] were performed using aug-cc-pVTZ basis set[27]; for comparison, density functional theory (DFT) calculations were also performed using the B3LYP exchange–correlation functional,[28,29] with the same basis functions. Optimizations of the open-shell species have been carried out using UHF methodology[30] and for closed-shell species, RHF methodology was used. It should be noted that negligible spin contaminations were observed. Harmonic vibrational frequencies were computed to evaluate the zero-point vibrational energy corrections, which have been included in all the reported energies in this work. It is notable that no imaginary frequencies were found for the reactants, product and the pre-reaction complex, which verify that they were all minima in the PES at all of the theoretical levels investigated in this work. Transition states were confirmed from the analysis of their frequencies, by ensuring only one imaginary frequency for each of those transition states. We have also carried out analysis of the displacement vectors for the imaginary frequencies of those transition states, to ascertain that the transition states were structurally true transition states and also confirmed them from their intrinsic reaction coordinates analysis.[31] It was

found that both MP2 and B3LYP methods predict similar kinds of trends for the PES, thus discussion reported in this work is limited only to the MP2(full) method, and the results related to the B3LYP method are provided in the Supporting Information. The basis set superposition error (BSSE), a source of error in supermolecular calculations, happens due to the finite size of the basis sets and has been accounted for the pre-reaction complex using the counterpoise correction of Boys and Bernardi.[32] To analyze the nature of interaction for one of the stationary points, we have carried out interaction energy decomposition analysis (commonly known as EDA[33]) implemented in the GAMESS software package.[34] The details of the input file used for this calculation are provided in the Supporting Information file.

3. Results and Discussions

3.1. *Electrostatic potentials of the reactants*

Computed ESP maps of the reactants, SO_2 and OH are shown in Fig. 1. Analysis of the ESP of SO_2 shows that the regions of the positive electrostatic potential are above and below the central atom (above and below the plane of SO_2). These positive regions are usually referred as π-holes.[35–39] In SO_2, accumulation of the π-holes above and below the S-atom can be explained as, "because of the more electronegative O-atoms, π-bonding electrons are drawn sufficiently towards the O-atoms, so that the associated rearrangement of the electronic density leaves a region of positive potentials above and below the S-atom".[39] Similarly, from Fig. 1, regions of negative electrostatic potentials can also be found around the two O-atoms of the SO_2

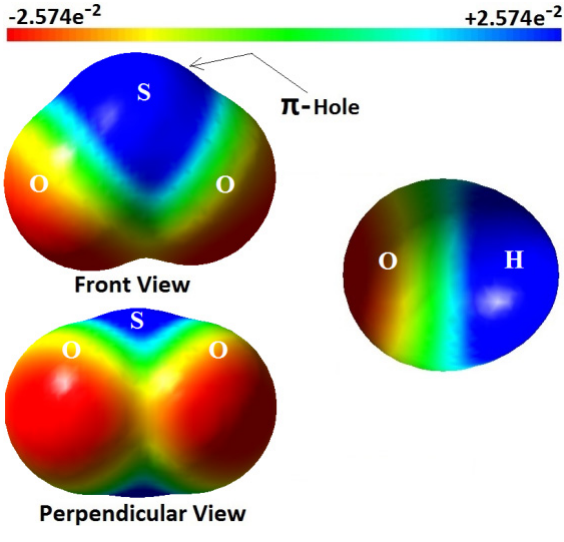

Fig. 1. Computed ESP maps of OH and SO_2 calculated from the MP2(full)/aug-cc-pVTZ method at 0.02 au electron density surfaces. Quantitative values of electrostatic potentials are also in au.

molecule and they are concentrated around the S-O bond axes. At the same time, analysis of the ESP maps of the OH fragment shows that there are positive electrostatic potentials around the H-atom and negative electrostatic potentials around the O-atom. Analyzing the ESP maps of OH and SO_2, one can say that when these two approach toward each other, there are two possibilities of favorable interaction. The first case in which the O-atom of the OH is oriented in such a way that it can favorably interact with the S-atom of the SO_2 and the second case in which the H-atom of the OH is oriented in such a way that it can favorably interact with the one of the O-atoms of the SO_2. Thus ESP maps of OH and SO_2 clearly indicate possible favorable interactions between the two.

3.2. *Approach of the reactants toward each other*

The two possibilities as discussed earlier have been investigated completely to find any possibilities of complexation between the OH and SO_2. In the first case, we have focussed on the approach of OH toward SO_2 where the H-atom of the OH is close to one of the O-atoms of the SO_2. The two possibilities of approaching of OH toward SO_2 along with the Lewis structure of SO_2 with the complete electronic arrangements around the atoms have been shown in Fig. 2. From the Lewis structure of SO_2, it is well known that both the oxygen atoms in the SO_2 molecule are symmetric in nature (as they are symmetrically situated with respect to the molecular C_2-axis) and hence approach of OH toward either O-atom will be equivalent. This is the reason behind why we have tried to visualize the approach of OH toward SO_2 only at one of the O-atoms of SO_2. Now, once the OH is close to one of these O-atoms of the SO_2 molecule, it is going to encounter some interaction with the two lone pairs of electrons present on the oxygen atom. But, the two lone pairs of electrons present on each oxygen atom of SO_2 are not equivalent due the geometric constraints. When OH approaches toward the SO_2 molecule to form a possible hydrogen-bonded complex, one can expect that the O-atom of the SO_2 acts as a donor and H-atom of OH acts as

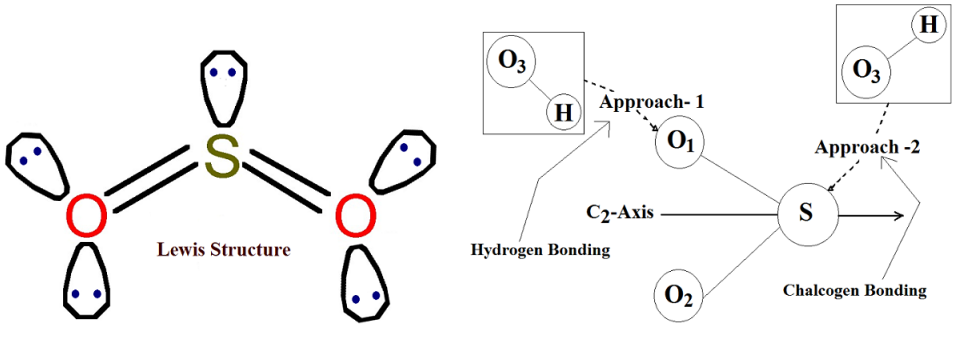

(a) (b)

Fig. 2. (a) Pictorial representation of the Lewis electronic structure of SO_2. (b) Schematic representation of the two possible ways of OH approaching toward SO_2.

an acceptor. The lone pairs on the O-atom of SO_2 have donating capabilities and also at the same time are not equivalent. Thus approach of OH toward O-atom of the SO_2 is subjected to result in two nonequivalent interaction modes. By applying valence shell electron pair repulsion (VSEPR) theory, one can easily predict that either of the two complexation modes will result in a trigonal planar arrangement around the O-atom of the SO_2 fragment. It is also well known that the interactions due to σ-holes and π-holes or in general interactions arising from the electrostatics are highly directional in nature owing to the anisotropic nature of the ESP distribution in most of the molecules.[35–39] Thus optimum care was taken while searching for an interaction possible hydrogen-bonded complex, and interestingly, we were able to locate one such complex in the PES. The optimized structure of the complex is shown in Fig. 3. Although there was a probability of existence of two possible hydrogen-bonded complexes, we were able to locate only this *cis*-type of hydrogen bonding interaction mode with a complete planar type of structural arrangement after lots of rigorous attempts. We know that the rules of the VSEPR theory are noncommittal with respect to the direction in which the OH is interacting with the SO_2. So, we assume that getting only the *cis* complexation mode in the PES can be attributed to the more nucleophilic nature of the *cis*-nonbonding electron pair of the O-atom of the SO_2 than the other lone pair.[40] From the complex, it can be seen that the computed geometry in fact agrees completely with the VSEPR theory prediction, e.g. the S-O-H angle is 154.6° (trigonal planar arrangement around the O-atom). Now, the O–H distance, which is 2.033 Å, is perfectly in the range of H-bonding distances. With the BSSE corrections, the complex was found to be around 4.2 kcal/mol more stable compared with the reactants.

In the second case is where the approach of OH is on the S-atom side (somewhat close/along the C_2-axis of the SO_2 molecule). Now in such a situation if the O-atom of OH favorably interacts with the S-atom of SO_2, then there is a possibility of

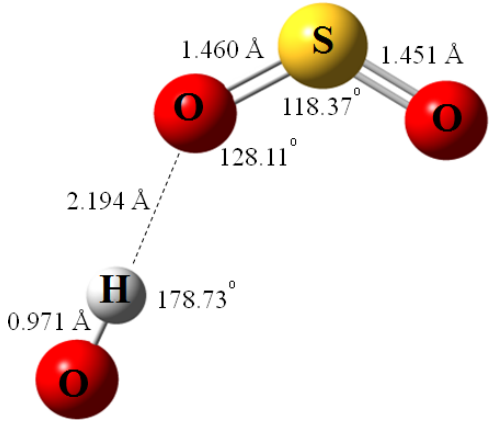

Fig. 3. Minimum energy structure of the pre-reaction hydrogen-bonded complex optimized using MP2 (full)/aug-cc-pVTZ. Important geometric parameters are also shown.

getting a complex with chalcogen interactions. Although the electrostatic potentials show it to be favorable (negative on the O-atom of the OH and positive on the S-atom of SO_2), our search was not able to locate any stationary points along this path despite numerous attempts. In some of the cases, our searches resulted in the transition state like structure with one imaginary frequency,[23] and in most of the cases, our searches ended in getting the product $HOSO_2$.

3.3. *Nature of interaction in the complex*

Analysis of structure of the pre-reaction complex shows that the type of interaction existing at the complex is of hydrogen bonding in nature. Hydrogen bonding types are often described as strong dipole–dipole interaction with the characteristic feature of directionality and are strongest types of Keesom interactions. So, we analyzed the resultant dipole moment of the complex and compared with the reactants. Our observations also indicate a perfect dipole–dipole type of interaction as there is an enhancement in the resultant dipole moment of the complex when compared with the dipole moments of the reactants. Also, the directionality aspect of this Keesom interaction can easily be addressed by considering the more constrained geometry of the pre-reaction complex. Although the analysis of the H-bonding distances indicates the H-bond strength to be medium ranged, complexation energy indicates that the strength of the H-bonding is in the lower range.[40] Such a situation indicates that in the PES the repulsive interactions are still dominant at this complexation distance. So to have an idea about the nature of interactions existing in the pre-reaction complex, we have carried out the interaction EDA.[33] The input file used for this calculation is provided in Supporting Information, and the results are shown in Table 1. As there were some convergence problems, EDA calculations implemented in GAMESS have been carried out using a lower basis set like 6-31G(d,p) with the unrestricted Hartree–Fock method.[34]

The total interaction energy calculated by this method was found to be −3.42 kcal/mol, indicating that the interaction is a favorable and stabilizing interaction. The quantitative value is slightly underestimated as the calculation was carried out at a lower level of theory. Although the total effect of the interaction between the OH and SO_2 is stabilizing, from the analysis of the interaction energy components, it can be observed that the repulsive component (+7.85 kcal/mol) is the largest component. We were not able to find any reasonable explanation to account for this large repulsive interaction term. At this point, we think that the large repulsion might be arising from the repulsion between the positive electrostatic

Table 1. Interaction EDA carried out using EDA method at HF/6-31G(d,p).

Electrostatic energy	−5.21 kcal/mol	Exchange energy	−4.37 kcal/mol
Repulsion energy	+7.85 kcal/mol	Polarization energy	−1.69 kcal/mol
Total interaction energy		−3.42 kcal/mol	

potentials of σ-hole with the positive electrostatic potentials around the H-atom. To support our view, geometry of the pre-reaction complex shows that the positioning of the H–O=S in the complex (128.11°: Fig. 3) along with the short bond distance of the O-H subunit making it to be placed very much close to the σ-hole region of the S=O bond. As expected from the electrostatic potential mapping of the reactants, there is a large attractive interaction term in the form of electrostatic energy (−5.21 kcal/mol). Besides this attractive term, there is a significant attractive contribution coming in the form of exchange energy (−4.37 kcal/mol) and also a substantial contribution in the form of polarization energy. The interaction energy decomposition qualitatively shows that although the total interaction energy is negative or stabilizing, there is a large positive repulsion interaction energy contribution to it and thus making the total interaction energy substantially low.

Also, to analyze the nature of orbital interactions existing when OH approaches toward the SO_2 to form the pre-reaction complex, we have constructed the orbital interaction diagram as shown in Fig. 4. From the EDA, it can be seen that the polarization energy is relatively small. This gives an indication that the frontier molecular orbitals (MOs) are not significantly perturbed. From Fig. 4, it can also be observed that the MOs of the pre-reaction complex are not significantly perturbed. In fact, the MOs LUMO and HOMO-1 seem to be rather localized MOs coming directly from the LUMO of SO_2 and HOMO-1 of OH, respectively. Though there are no significant MO perturbations observed in the pre-reaction complex compared with the reactant MOs, we have observed a significant MO overlap between the HOMO of OH and HOMO of SO_2. In the EDA, the relatively large value of the repulsion energy also gives an indication of the significant MO overlap. Overlap of the HOMOs of OH

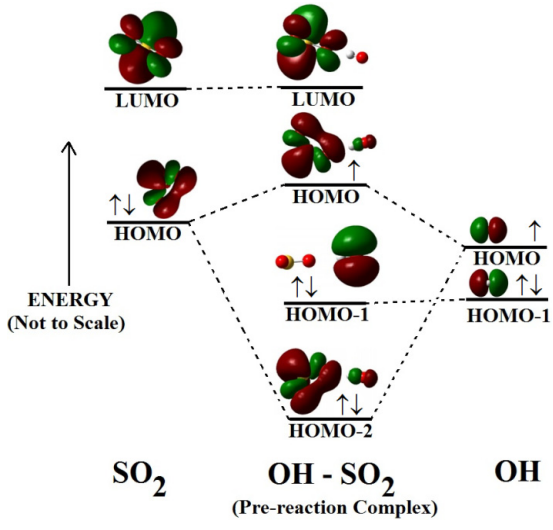

Fig. 4. Frontier molecular orbital interaction diagram for the pre-reaction complex formation from OH and SO_2 (MP2(full)/aug-cc-pVTZ geometries were used to get the frontier molecular orbitals).

and SO_2 resulted in two MOs of the pre-reaction complex, viz., HOMO and HOMO-2 of the pre-reaction complex. Analysis of these two frontier MOs of the pre-reaction complex shows that, in the process of the orbital mixing, the maximum contributions are from the MOs of SO_2.

3.4. *PES of OH + SO_2→ $HOSO_2$*

The reaction between OH and SO_2 is a crucial reaction in the atmosphere as it is believed to be the rate-limiting reaction in the atmospheric formation of H_2SO_4.[1–5] Owing to its importance, this reaction has been studied experimentally as well as theoretically by many research groups.[6–16] But, there still exists a long standing debate in the literature, whether this reaction is really barrier-less or passes through a small barrier. For example, the experimental work of Wine *et al.*[40] suggests a barrier-less PES (based on their K_1^∞ measurement, they report a slight decrease in K_1^∞ value with the increase in the temperature), whereas on the contrary, the experimentally determined K_1^∞ by Fulle *et al.*[21] indicates the presence of a barrier in the PES of the OH and SO_2 reaction (K_1^∞ measured by Fulle *et al.* over a range of 1–96 bars showed an increase in the rate constant value with increasing temperature).

The PES of this reaction has been studied computationally by Li and McKee[41] and Somnitz.[22] The reported values for the enthalpy of this reaction by these authors are −109.6 kJ/mol (Li and McKee[41]) and −109.3 kJ/mol (Somnitz[22]), which are in good agreement with the calculated value of −109.2 kJ/mol in this work and also at the same time are very much close to the experimentally reported value of -113.3 ± 6 kJ/mol at 298 K.[42] Besides the thermochemistry data, the experimentally reported vibrational frequencies (four different vibrations observed experimentally have been reported in the literature[40,43]) for $HOSO_2$ are also very close to the computed frequencies in this work (Supporting Information). Li and McKee[41] were not able to locate a true transition state, whereas Somnitz[22] was able to locate a small barrier for this reaction. Before the report of Somnitz,[22] Moore-Plummer *et al.*[44] were also able to locate a small barrier for this reaction in both DFT and MP2 methods. Glowacki *et al.*[45] carried out a relaxed PES scan along the HO–SO_2 bond, using UB3LYP/aug-cc-PVQZ level of theory to show the possible presence of a barrier for this reaction. In a recent extensive study of this reaction and also kinetics of this reaction by Long *et al.*,[46] they were also able to locate a small reaction barrier. In this recent work also, presence of such a pre-reaction complex, which is the focus of this work, is not discussed.

In the reaction path, there are two reactants, viz., OH and SO_2 pass through a pre-reaction complex and transition state to reach the product, $HOSO_2$. Both the reactants are neutral in nature with the reactant OH having radical characteristics. The neutral product, $HOSO_2$, is also radical in nature. The OH radical is in $C_{\infty v}$ symmetry (linear) and has a doublet $^2\Sigma$ state. The stable neutral SO_2 is C_{2v} symmetric and is in a singlet $^1A_1$ state. The structure of the SO_2 is planar and bent.

Analysis of the vectorial dipole components of both the reactant molecules shows that the dipole vectors of both the molecules have the largest magnitude in the z-direction. Spin density analysis of the OH shows that the total spin of the one unpaired electron resides on the O-atom. Note that there is very little spin contamination found in the optimization of the OH radical. For $HOSO_2$, it was observed that the molecule is in a doublet ground state with gauche conformation (state ^2A) and C_1 symmetry (note that there is very little spin contamination found in the optimization of the $HOSO_2$ radical). Analysis of the spin density shows that the spin density on the OH fragment is largely reduced and the maximum spin density is accumulated on the SO_2 fragment (distributed over the S-atom and O-atoms). This clearly shows almost complete spin density transfer from the OH to the SO_2 in the formation of $HOSO_2$.

Analysis of the geometries of the pre-reaction complex and the transition state shows that while in the pre-reaction complex OH and SO_2 have a full planar type of structural arrangements (two-dimensional structural arrangement), these two reactants have a three-dimensional (3D) type of structural arrangement in the transition state with the OH being placed above the SO_2 plane (the OH group is above the molecular plane of the SO_2 and in a pseudo parallel fashion to S–O bond). Further analysis of the structure of the transition state indicates that the O–H bond is not completely parallel to S–O bond rather there is a twisting angle between the two. This can be explained by considering the short O–H distance, by which the H-atom is experiencing repulsions from the positive π-hole region around the S-atom, and such a situation is consistent with the disposition of the molecular electrostatic potentials of the constituent fragments. Analysis of both the structures also shows that there is a very little change in the O–S–O bond angle during the progress of this transformation. Such kind of behavior gives a clear indication that the O–S–O bending mode acts as a spectator and does not undergo transition to a higher vibrational state when the OH fragment approaches toward it, i.e. SO_2 still retains its ground state.[47] On the contrary, since OH rotor has a very low moment of inertia compared with SO_2, for any change in the potential, the response of OH in adjusting its position will be prominent.[47] As there is a change in the potential in moving from the complex to the transition state, the 2D structure of the pre-reaction complex has now changed to the 3D transition state structure and the only significant observable change is the position of OH. We have also observed that for the atomic spin density of the fragment, OH is conserved on the OH fragment for the transition state as well as the pre-reaction complex. We have also analyzed the imaginary frequency of the transition state and found it to be $368.3i\,cm^{-1}$. It is well known that one can have some qualitative information about the width of a barrier from its imaginary frequency. In other words, the quantitative value of the imaginary frequency gives a qualitative idea about the width of the barrier. It is well known that lower values of the transition state imaginary frequencies are associated with gentler, broader barriers, whereas higher values correspond to sharper, narrower barriers.[48] The imaginary frequency observed for the transition state is truly very small, and this clearly

indicates that the barrier is definitely broader. Now comparing the geometry of the TS with the complex and product, one can say that in moving from the complex to the TS and from there to the product comprises huge structural changes. Moving from the complex to the TS in the geometric space means a transition from 2D all planar type of orientation of the reactants to the parallel 3D orientation of the reactants. Similarly, a move from the TS to product indicates an incomplete movement back to the 2D type of arrangement (the structure of the product, $HOSO_2$, has a slightly pyramidal type of structural arrangement). In our view of such an oscillation in the geometries of the stationary points, it can be said that it is not only going to broaden the TS width but also capable of slowing down the transformation process. In light of this view, we can say that Step 2 might be regarded as the slowest step between the two steps. In such a scenario as discussed earlier, the increase in the barrier height due to the presence of a pre-reaction complex may affect the kinetics of reaction 1. In other ways, we can also say that the effect of this pre-reaction complex might be marginal, but might have a strong effect on the reaction dynamics.

The reaction path for the reaction between OH and SO_2 is shown in Fig. 5. It can be seen that the pre-reaction complex is a potential well located between the reactants and the transition state. This hydrogen-bonded complex was found to be 4.2 kcal/mol (2.1 kcal/mol, without the ZPE corrections) more stable than the reactants. Presence of the barrier brings out lots of changes to the PES of this reaction. First, as the reaction proceeds through such a complex formation, the barrier height for this reaction is almost raised two-fold (now the barrier heights are 9.5 kcal/mol and 6.9 kcal/mol without the ZPE corrections) to reach the product. Thus we can say that the presence of this complex increased the barrier height to a

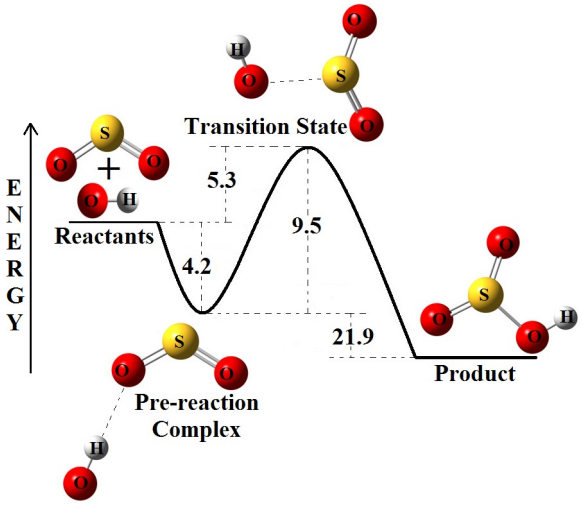

Fig. 5. Computed PES generated from the energies of the corresponding stationary points at MP2(full)/aug-cc-pVTZ.

measurable amount compared with the case of the PES where no such complex exists as reported earlier by Sitha *et al.*[23]

To check the effect of higher level calculations on the energies of the stationary points in the reaction path, we tried to do the single point energy calculations using the CCSD(T)/aug-cc-pVTZ method[49–51] on the MP2(full)/aug-cc-pVTZ optimized geometries. It is interesting to mention here that the pre-reaction complex, which was 2.1 kcal/mol below the reactants (without ZPE corrections) in the MP2 method, is now only 1.4 kcal/mol below the reactants. Other interesting observation to mention is that the transition state is now also below the reactants (0.5 kcal/mol below the reactants), but it can still be considered as a transition state, as it was found to be 0.9 kcal/mol above the pre-reaction complex. When we calculated the enthalpy of formation for the reaction, it was found to be −98.8 kcal/mol. When compared this with the value of enthalpy calculated at MP2(full)/aug-cc-pVTZ (−109.2 kJ/mol in this work) and with that of the experimentally reported value of -113.3 ± 6 kJ/mol at 298 K,[42] we observed that the thermodynamic data from the single point CCSD(T)/aug-cc-pVTZ method seem to be underestimated. Due to limited computing facilities available with us, we were not able to perform the full optimization using the CCSD(T) method.

Presence of the pre-reaction complex as a potential well in the PES may affect the kinetics of this reaction. With the presence of the pre-reaction complex, the complete reaction path can now be treated as a two-step process, in which Step 1 will be the formation of this super-molecule and Step 2 will be the transformation of this super-molecule to the product via the transition state.

$$\mathrm{OH} + \mathrm{SO_2} \rightarrow \mathrm{HO-SO_2} \quad \text{(Step 1)}$$
$$\mathrm{HO-SO_2} \rightarrow \mathrm{HOSO_2} \quad \text{(Step 2)}$$

Step 1 is a bi-molecular reaction, whereas Step 2 is a unimolecular reaction. Now the overall kinetics of this reaction will be decided based on the fact that between these two steps, which one is the slowest step. If Step 2 will be the slowest step, then the increase in the barrier height is definitely going to affect the kinetics of the reaction substantially by affecting the exponential factor of the Arrhenius equation [$k(T) = Ae^{-\frac{E_a}{RT}}$] (where E_a is an experimental parameter related to the overall barrier height for the reaction and A is the pre-exponential factor). In contrast, if Step 1 will be the slowest step, then how it is going to affect the kinetics of the overall reactions cannot be projected with the energetics data available with us. We can predict that the number density of the reactants, OH and SO_2 in the atmosphere and/or the pre-exponential factor 'A' (not possible to estimate theoretically) might be the contributing factors. But, if Step 2 becomes the slowest step, then it will be easy for us to predict the kinetic behavior of reaction 1. Unfortunately, we were not able to calculate the rate constant for this reaction in this work (as the reaction paths show multiple wells) to compare directly with the rate constant values reported in the literature and at the same time to have a quantitative assessment of the role of

pre-reaction complex on the kinetics of the overall reaction. Classical nuclear molecular dynamics calculations and systematic kinetics calculations using master equations will be of great help to completely understand the fate of this atmospherically important reaction.

4. Conclusions

In conclusion, for the first time, we were able to locate a stable hydrogen-bonded pre-reaction complex in the PES of the reaction between OH and SO_2. We found that this pre-reaction complex is a potential well between the reactants and transition state in the PES. We have analyzed the nature of interactions existing in the complex from the electrostatic potential maps of the reactants and also from the interaction EDA of the pre-reaction complex. Our interaction decomposition analysis shows that though the interacting surface between OH and SO_2 is attractive from the electrostatic point of view, it is also repulsive and the repulsive interaction may be due to the electrostatic interactions arising from the positive potentials of the σ-hole of the S=O σ-bond with the positive electrostatic potentials present around the H-atom of the OH fragment. After finding the pre-reaction complex, it has been shown that the reaction between the OH and SO_2 goes through a two-step process, in which the first step is the formation of the pre-reaction complex and the second step is the transformation of this pre-reaction complex to the product over the transition state. We have also compared the geometry of the pre-reaction complex with the geometries of the transition state and the product. We found that the presence of this pre-reaction complex in the PES creates a geometric constraint by the directionality nature of the hydrogen bonding and renders no geometric synergy between the TS and product. This lack of synergy in the orientations or geometries between the pre-reaction complex to the transition state to the product might be responsible not only for the broadening of the transition state width, but also compelling the reaction to go slow. Based on this argument, we have proposed that the step involving the transformation of the pre-reaction complex to the product might be the slowest step, and thus increase in the barrier height due to the presence of the pre-reaction complex might be able to affect the kinetics of the reaction by slowing it down further. As we were not able to perform the rate constant calculations for this reaction, at this stage, we are not sure how such a pre-reaction complex might affect the kinetics of the overall reaction. Therefore, a detailed calculation of the rate constant for reaction 1 will be able to quantitatively ascertain the role of the pre-reaction complex in affecting the kinetics of the reaction.

Acknowledgments

The authors like to thank University of Johannesburg for the support. The calculations reported here are carried out at the Centre for High Performance

Computing (CHPC), South Africa and the authors like to thank CHPC for providing the facility. S.S. thanks the NRF, South Africa for incentive funding. Z.P.N. thanks NRF, South Africa for PhD bursary. V.M.M. thanks University of Johannesburg for the Postdoctoral fellowship. P.B. thanks University of Johannesburg for the PhD bursary.

Supporting Information

Total energies of all the stationary points located in the reaction PES calculated using other methods are provided in Table S1. Electrostatic potential maps of the pre-reaction complex and the transition state are provided in Fig. S1. Besides, these optimized Cartesian coordinates and all other important physical data for all the stationary points have also been provided. A GAMESS input file used for the interaction EDA calculation is also provided.

References

1. Calvert JG, Fu S, Bottenheim JW, Strauz OP, Mechanism of the homogeneous oxidation of sulfur dioxide in the troposphere, *Atmos Environ* **12**:197–226, 1978.
2. Calvert JG, Lazrus A, Kok GL, Heikes BG, Walega JG, Lind J, Cantrell CA, Chemical mechanisms of acid generation in the troposphere, *Nature* **317**:27–38, 1985.
3. Margitan JJ, Mechanism of the atmospheric oxidation of sulfur dioxide. Catalysis by hydroxyl radicals, *J Phys Chem* **88**:3314–3318, 1984.
4. Calvert JG, Stockwell WR, in Calvert JG, Teasley JI (eds.), *SO_2, NO and NO_2 Oxidation Mechanisms: Atmospheric Considerations. Acid Precipitation Series 3*, Butterworth Publishers, Boston, MA, 1984.
5. Kuo Y-P, Cheng B-M, Lee Y-P, Production and trapping of $HOSO_2$ from the gaseous reaction OH + SO_2: The infrared absorption of $HOSO_2$ in solid argon, *Chem Phys Lett* **177**:195–199, 1991.
6. Harris GW, Wayne RP, Reaction of hydroxyl radicals with NO, NO_2 and SO_2, *J Chem Soc Faraday Trans* **1**:610–617, 1975.
7. Castleman Jr AW, Tang IN, Kinetics of the association reaction of SO_2 with the hydroxyl radical, *J Photochem* **6**:349–354, 1977.
8. Leu MT, Rate constants for the reaction of hydroxyl with sulfur dioxide at low pressure, *J Phys Chem* **86**:4558–4562, 1982.
9. Martin D, Jourdain JL, Le Bras G, Discharge flow measurements of the rate constants for the reaction OH + SO_2+ He and $HOSO_2$+ O_2 in relation with the atmospheric oxidation of sulfur dioxide, *J Phys Chem* **90**:4143–4147, 1986.
10. Lee YY, Kao WC, Lee YP, Kinetics of the reaction hydroxyl + sulphur dioxide in helium, nitrogen, and oxygen at low pressure, *J Phys Chem* **94**:4535–4540, 1990.
11. Atkinson R, Perry RA, Pitts JN, Rate constants for the reactions of the OH radical with NO_2 (M 1/4 Ar and N_2) and SO_2 (M 1/4 Ar), *J Chem Phys* **65**:306–310, 1976.
12. Paraskevopoulos G, Singleton DL, Irwin RS, Rates of OH radical reactions. The reaction OH + SO_2+ N_2, *Chem Phys Lett* **100**:83–87, 1983.
13. Davis DD, Ravishankara AR, Fischer S, SO_2 oxidation via the hydroxyl radical: Atmospheric fate of HSOx radicals, *Geophys Res Lett* **6**:113–116, 1979.
14. Cox RA, Sheppard D, Reactions of OH radicals with gaseous sulphur compounds, *Nature* **284**:330–331, 1980.

15. Izumi K, Mizuochi M, Yoshioka M, Murano K, Fukuyama T, Redetermination of the rate constant for the reaction of hydroxyl radicals with sulphur dioxide, *Environ Sci Technol* **18**:116–118, 1984.
16. Leung FY, Colussi AJ, Hoffmann MR, Sulfur isotopic fractionation in the gas-phase oxidation of sulfur dioxide initiated by hydroxyl radicals, *J Phys Chem A* **105**:8073–8076, 2001.
17. Criegee R, Wenner G, Die ozonisierung des 9, 10-oktalins, *Liebigs Ann Chem* **564**:9–15, 1949.
18. Chhntyal-Pun R, Davey A, Shallcross DE, Percival CJ, Orr-Ewing A, A kinetic study of the CH_2OO Criegee intermediate self-reaction, reaction with SO_2 and unimolecular reaction using cavity ring-down spectroscopy, *Phys Chem Chem Phys* **17**:3617–3626, 2015.
19. Welz O, Savee JD, Osborn DL, Vasu SS, Percival CJ, Shallcross DE, Taatjes CA, Direct kinetic measurements of Criegee intermediate (CH_2OO) formed by reaction of CH_2I with O_2, *Science* **335**:204–207, 2012.
20. Mauldin RLIII, Berndt T, Sipila M, Paasonen P, Petaja T, Kim S, Kurten T, Stratmann F, Kerminen VM, Kulmala M, A new atmospherically relevant oxidant of sulphur dioxide, *Nature* **488**:193–196, 2012.
21. Fulle D, Hamann HF, Hippler H, The pressure and temperature dependence of the recombination reaction HO + SO_2+ M → $HOSO_2$+ M, *Phys Chem Chem Phys* **1**:2695–2702, 1999.
22. Somnitz H, Quantum chemical and dynamical characterisation of the reaction OH +SO_2 ⟷ $HOSO_2$ over an extended range of temperature and pressure, *Phys Chem Chem Phys* **6**:3844–3851, 2004.
23. Sitha S, Jewell LL, Piketh SJ, Fourie G, A quantum chemical calculation of the potential energy surface in the formation of $HOSO_2$ from OH + SO_2, *Atmos Environ* **45**:745–754, 2011.
24. Frisch MJ, Trucks GW, Schlegel HB, Scuseria GE, Robb MA, Cheeseman JR, Scalmani G, Barone V, Mennucci B, Petersson GA, Nakatsuji H, Caricato M, Li X, Hratchian HP, Izmaylov AF, Bloino J, Zheng G, Sonnenberg JL, Hada M, Ehara M, Toyota K, Fukuda R, Hasegawa J, Ishida M, Nakajima T, Honda Y, Kitao O, Nakai H, Vreven T, Montgomery JA Jr., Peralta JE, Ogliaro F, Bearpark M, Heyd JJ, Brothers E, Kudin KN, Staroverov VN, Kobayashi R, Normand J, Raghavachari K, Rendell A, Burant JC, Iyengar SS, Tomasi J, Cossi M, Rega N, Millam JM, Klene M, Knox JE, Cross JB, Bakken V, Adamo C, Jaramillo J, Gomperts R, Stratmann RE, Yazyev O, Austin AJ, Cammi R, Pomelli C, Ochterski JW, Martin RL, Morokuma K, Zakrzewski VG, Voth GA, Salvador P, Dannenberg JJ, Dapprich S, Daniels AD, Farkas O, Foresman JB, Ortiz JV, Cioslowski J, Fox DJ, Gaussian 09, Gaussian, Inc., Wallingford, CT, 2009.
25. Frisch MJ, Head-Gordon M, Pople JA, Direct MP2 gradient method, *Chem Phys Lett* **166**:275–280, 1990.
26. Frisch MJ, Head-Gordon M, Pople JA, Semi-direct algorithms for the MP2 energy and gradient, *Chem Phys Lett* **166**:281–289, 1990.
27. Dunning TH Jr., Gaussian basis sets for use in correlated molecular calculations. I. The atoms boron through neon and hydrogen, *J Chem Phys* **90**:1007–1023, 1989.
28. Becke AD, Density-functional thermochemistry. III. The role of exact exchange, *J Chem Phys* **98**:5648–5652, 1993.
29. Lee C, Yang W, Parr RG, Development of the Colle–Salvetti correlation-energy formula into a functional of the electron density, *Phys Rev B* **37**:785–789, 1988.
30. McWeeny R, Dierksen G, Self-consistent perturbation theory. 2. Extension to open shells, *J Chem Phys* **49**:4852, 1968.

31. Hratchian HP, Schlegel HB, Accurate reaction paths using a Hessian based predictor-corrector integrator, *J Chem Phys* **120**:9918–9924, 2004.
32. Boys SF, Bernardi F, Calculation of small molecular interactions by differences of separate total energies — Some procedures with reduced errors, *Mol Phys* **19**:553, 1970.
33. Su P, Li H, Energy decomposition analysis of covalent bonds and intermolecular interactions, *J Chem Phys* **131**:014102/1–15, 2009.
34. Schmidt MW, Baldridge KK, Boatz JA, Elbert ST, Gordon MS, Jensen JH, Koseki S, Matsunaga N, Nguyen KA, Su S, Windus TL, Dupuis M, Montgomery JA, General atomic and molecular electronic structure system, *J Comput Chem* **14**:1347–1363, 1993.
35. Pal R, Nagendra G, Samarasimhareddy M, Sureshbabu VV, Guru Row TN, *Chem Commun* **51**:933, 2015.
36. Solimannejad M, Ramezani V, Trujillo C, Alkorta I, Sanchez G, Elguero J, *J Phys Chem A* **116**:5199, 2012.
37. Bauza A, Mooibroek TJ, Frontera A, The bright future of unconventional σ/π-hole interactions, *Chem Phys Chem* **16**:2496, 2015.
38. Bhasi P, Nhlabatsi ZP, Sitha S, Expanding the applicability of electrostatic potentials to the realm of transition states, *Phys Chem Chem Phys* **18**:13002–13009, 2016.
39. Murray JS, Lane P, Clark T, Riley KE, Politzer P, Σ-holes, π-holes and electrostatically-driven interactions, *J Mol Model* **18**:541–548, 2012.
40. Wine PH, Thompson RJ, Ravishankara AR, Semmes DH, Gump CA, Torabi A, Nicovich JM, Kinetics of the reaction OH + SO_2+ M → $HOSO_2$+ M, Temperature and pressure dependence in the fall-off region, *J Phys Chem* **88**:2095–2104, 1984.
41. Li W-K, McKee ML, Theoretical study of OH and H_2O addition to SO_2, *J Phys Chem A* **101**:9778–9782, 1997.
42. Blitz MA, Hughes KJ, Pilling MJ, Determination of the high-pressure limiting rate coefficient and the enthalpy of reaction for OH + SO_2, *J Phys Chem A* **107**:1971–1978, 2003.
43. Majumdar D, Kim G-S, Kim J, Oh KS, Lee JY, Kim KS, Choi WY, Lee S-H, Kang M-H, Mhin BJ, *Ab initio* investigations on the $HOSO_2$+ O_2 → SO_3+ HO_2 reaction, *J Chem Phys* **112**:723–730, 2000.
44. Moore-Plummer PL, Wu R, Flenner JJ, *Ab initio* investigation of the gas phase reaction SO_2+ H_2O → SO_2OH radical, *Mol Phys* **100**:1847–1853, 2002.
45. Glowacki DR, Reed SK, Pilling MJ, Shalashilin DV, Martinez-Nunez E, Classical, quantum and statistical simulations of vibrationally excited $HOSO_2$: IVR, dissociation, and implications for OH + SO_2 kinetics at high pressures, *Phys Chem Chem Phys* **11**:963–974, 2009.
46. Long B, Bao JL, Truhlar DG, Reaction of SO_2 with OH in the atmosphere, *Phys Chem Chem Phys* **19**:8082–8090, 2017.
47. Legon AC, Millen DJ, Angular geometries and other properties of hydrogen bonded dimers: A simple electrostatic interpretation of the success of the electron–pair model, *Chem Soc Rev* **16**:467–498, 1987.
48. Shannon RJ, Blitz MA, Goddard A, Heard DE, Accelerated chemistry in the reaction between the hydroxyl radical and methanol at interstellar temperatures facilitated by tunnelling, *Nat Chem* **5**:745–749, 2013.
49. Scuseria GE, Janssen CL, Schaefer HF III, An efficient reformulation of the closed-shell coupled cluster single and double excitation (CCSD) equations, *J Chem Phys* **89**:7382–7387, 1988.
50. Purvis GD III, Bartlett RJ, A full coupled-cluster singles and doubles model — The inclusion of disconnected triples, *J Chem Phys* **76**:1910–1918, 1982.
51. Scuseria GE, Schaefer HF III, Is coupled cluster singles and doubles (CCSD) more computationally intensive than quadratic configuration-interaction (QCISD)? *J Chem Phys* **90**:3700–3703, 1989.